Proceedings of the Institution of Civil Engineers
Structures and Buildings 162
August 2009 Issue SB4
Pages 221–232
doi: 10.1680/stbu.2009.162.4.221

Paper 800078
Received 22/10/2008
Accepted 13/05/2009

Keywords: cables & tendons/ composite structures/strength and testing of materials

Ioannis P Giannopoulos
Department of Engineering, University of Cambridge, UK

Chris J Burgoyne
Department of Engineering, University of Cambridge, UK

ice
Institution of Civil Engineers

Stress limits for aramid fibres

I. P. Giannopoulos Dipl. Civil Eng., MSc, DIC, PhD and C. J. Burgoyne MA, MSc, PhD, DIC, CEng, MICE, FIStructE

Aramid fibres should have many structural applications: they should be used as tendons in prestressed concrete, as stay cables in bridges and as ropes in marine industry owing to their good tensile properties, low weight and lack of corrosion. However, uncertainty about their ability to carry significant loads for a long period of time has meant that engineers have been reluctant to adopt them. Two new techniques (stepped isothermal method and stepped isostress method) are now available that allow accelerated testing to be carried out at low stress levels, in such a way that the long-term creep and creep rupture properties can be determined without having to extrapolate more than one decade on a log-time scale. Such tests have now been carried out on two slightly different aramid fibres: Kevlar 49 and Technora. The paper shows how this information can be used to predict the safe operating stresses for these fibres when under sustained load, which is precisely the sort of application for which they are most economically suited. The effects of yarn variability are considered, as are the effects of different temperatures and varying loads. The aim is to be able to predict the behaviour of aramid fibres when subject to load durations of 100 years or more, without having to provide excess material because of a lack of applicable test data.

NOTATION

A	cross-sectional area
ABL	average breaking load
CCT	conventional creep tests
E	activation energy
f_{fd}	design strength of fibre
f_{fk}	characteristic strength of fibre
f_u	ultimate strength
n	influence term
P	load
SIM	stepped isothermal method
SSM	stepped isostress method
T	temperature
T_{eff}	effective temperature
T_R	reference temperature
t_r	rupture time
R	universal gas constant
R_{10}	reduction in strength per decade (%)
RH	relative humidity
α_T	shift factor for temperature
$\eta_{env,t}$	environmental strength reduction factor
μ	mean value
σ	standard deviation

1. INTRODUCTION

Composite materials have been considered for use in structures for more than 20 years. Fibres such as aramid, carbon and glass have become increasingly popular in many structural applications owing to their unique mechanical properties. They possess a combination of high strength, high stiffness and good resistance to creep and corrosion. External and internal prestressing, strengthening of structures through composite plates, composite bars as reinforcement, composites in the marine and railway industries and in ground engineering are some of the areas where fibrous composites can be used. A detailed review of the applications of different types of composites can be found elsewhere.[1]

The scope of this paper is limited to aramid fibres. Aramids can be used as tendons in prestressed concrete, as stay cables in bridges and as ropes in the marine industry, and for a number of other structural applications.[2] The main attraction is their good resistance to corrosion by water, which would allow their use as external tendons or with much reduced concrete cover. However, uncertainty about their ability to carry significant loads for a long period of time (stress–rupture) has meant that engineers have been reluctant to adopt them. Prestressing tendons in concrete are most susceptible to this type of failure because they are tensioned against concrete immediately after the concrete has hardened, to provide the required compressive stresses, and the high force remains in place for the lifetime of the structure.

Tendons are the most heavily stressed elements in any structure, with typical force in steel tendons reaching 70% of the average breaking load (ABL). However, creep of concrete and relaxation of the tendons will reduce that figure to about 60% ABL after a few months, after which it remains constant.[3] Until recently, only high-strength steel tendons have been used for prestressing concrete with ultimate tensile strengths reaching 1700 MPa. Aramids have a typical tensile strength about 3000 MPa, as shown in Figure 1. Aramids are tougher than carbon, so are easier to grip in a prestressing anchorage;[4] they therefore make an ideal material for use in prestressed concrete.

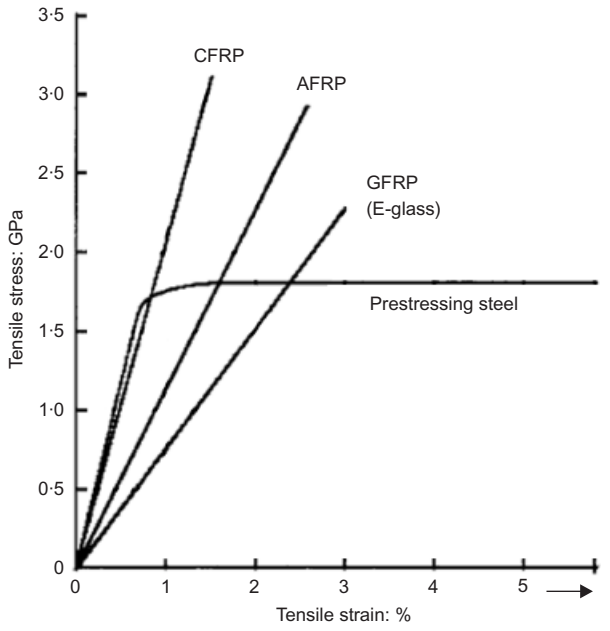

Figure 1. Stress–strain curves for aramid fibre reinforced polymer compared with prestressing steel[1]

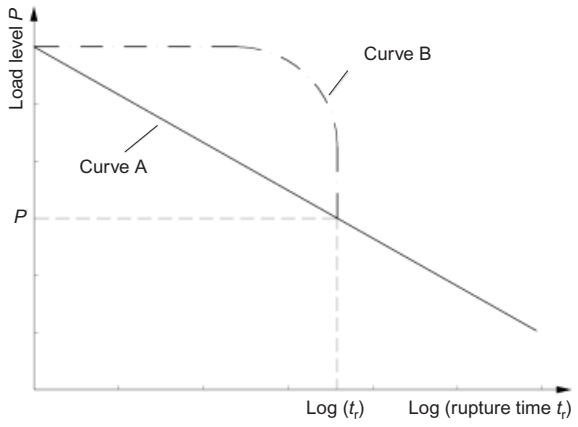

Figure 2. Stress–rupture (curve A) and residual strength (curve B) for aramid fibres

At the present time, aramid tendons are several times more expensive than steel. However, their good resistance to corrosion and the consequent assurance of long-term durability can compensate for the additional first cost if the whole-life costing is considered.[5] The whole-life cost is closely related to the allowable long-term stress that can be applied to the tendons, which is governed by the stress–rupture relationship.

According to most design codes and guidelines, the common design lifetime for residential or office buildings is 50 years and for bridges is 120 years. These figures are notional and very often society feels aggrieved if buildings or bridges need to be refurbished as a result of durability failures at any age. On the other hand, it is impossible to conduct tests for these durations before using new materials. Tests carried out in testing machines rarely last for more than a few days because of the expense of tying up the machine, while tests using dead weights have high capital costs and take up valuable space. Therefore, the only way to assess new materials to determine the design life is to apply extrapolation techniques to short-term test data.

2. STRESS–RUPTURE

Many materials exhibit stress–rupture behaviour, in which the material will eventually creep to failure if a high load is applied continuously. It is not normally a problem for steel at ambient temperatures, or for concrete, but glass and most organic materials are viscoelastic and typically exhibit such behaviour. For most materials in which viscoelasticity is a thermally activated process, following the Arrhenius equation, a linear relationship between the load and the logarithm of the time to failure can be expected (curve A in Figure 2). This curve does not, however, represent a decline in the short-term strength. If many specimens were loaded with a force P and then subsequently tested at different ages, up to the predicted rupture time t_r, the retained strength can be expected to follow curve B in Figure 2, showing that the short-term strength is not significantly reduced.[6]

Stress–rupture behaviour is distinct from other durability concepts such as hydrolysis and chemical attack and it does not imply that an unloaded specimen would be weaker after storage.

Engineers need predictions of the stress–rupture lifetime relationship together with associated probabilities-of-failure of the material. This has been a problem for the use of aramids because existing test data are limited to a few months, while the contemplated load durations may be over a century. A commonly held view is that extrapolations should only be made for one decade on the log-time scale. If longer extrapolations are made, much larger safety factors are frequently applied, which lower the perceived strength of the material. Nowadays, industry must evaluate both the real risk, owing to material variability, and the notional risk, owing to uncertainty in the modelling. Doubt in the extrapolation method can thus have a very real economic effect and can mean that a less suitable material is used simply because there is more confidence about its properties.

There is still an open debate about how design values should be obtained from the stress–rupture relationships. A commonly held approach is to obtain the characteristic value of the material at the prescribed design life and divide it by a partial safety factor. This factor for aramid fibres is proposed in some European design guides[7–9] to be in the range between the value used for steel and that used for concrete. Because there is no significant difference between the aramids in production, as well as in failure modes, a material partial safety factor of 1·25 is proposed by FIB.[10] However, this factor can be higher if there is doubt about the applied extrapolation technique.

2.1. Stress limits proposed by various researchers

Many researchers have examined the stress–rupture behaviour of aramid fibres and have recommended their own stress limits. Ferer and Swenson[11] recommended empirically a safety factor of 5 for ropes of Kevlar fibres, but they were contemplating marine rope applications where there is significant uncertainty in the loading. Prestressed tendons always have much lower factors of safety because the loading is under direct

engineering control. Guimaraes[12] conducted creep tests on parallel-lay aramid ropes; he determined a relationship between creep and rupture time, and proposed a stress limit of 0·54 f_u after 50 years. Yamaguchi *et al.*[13] carried out creep tests for 1000 h on fibre-reinforced plastic (FRP) rods made with aramid fibres and found a critical stress due to stress–rupture of 0·47 f_u after 50 years. Ando *et al.*[14] tested tendons made from aramid fibres and found a critical stress of 0·66 f_u after 50 years. Gerritse and Taerwe[15] proposed limiting the initial stress in prestressing elements to 0·55 f_u. Alwis and Burgoyne[16] tested aramid yarns at 50% and 70% ABL using accelerated techniques and found a stress limit of 0·64 f_u for 50 years. All stress limits for a service life of 50 years from various researchers are summarised in Table 1.

However, these creep–rupture predictions are based on conventional creep tests at ambient conditions and at high load levels (min. 70% ABL), when creep failures can be obtained in a short period of time. For lower stress levels extrapolation techniques have been used. The degree of extrapolation and the lack of test data introduce many uncertainties and therefore engineers should be very careful when using these figures in real structures.

2.2. Stress limits by design codes and guidelines

Currently, design guides for FRP reinforcement exist in Japan, Canada, Italy, the USA and the UK. In Norway, provisional design recommendations have been developed. Table 2 summarises the strength reduction factors used in international guidelines or codes to allow for environmental actions and sustained load.

The design guidelines of the British Institution of Structural Engineers (IStructE)[17] propose only one factor that reduces the material strength and this takes into account the effects of environment, sustained stress and other general uncertainties of the material.

	Stress limits for a service life of 50 years
Guimaraes[12]	0·54f_u
Yamaguchi *et al.*[13]	0·47f_u
Ando *et al.*[14]	0·66f_u
Gerrtise and Taerwe[15]	0·55f_u
Alwis and Burgoyne[16]	0·64f_u

Table 1. Recommended stress limits for aramid fibres from various researchers

Guidelines or codes	Reduction factor (% of the short-term tensile strength)	
	Environmental deterioration	Sustained load
ACI 440	0·80–0·90	0·24–0·27
ISE	0·50	
CHBDC	0·6	0·35–0·40
CNR	0·80–0·90	0·50
JSCE	0·87	⩽0·70
NS 3473	0·90	Not specified

Table 2. Recommended stress limits for aramid fibres from various guidelines and codes

On the other hand, other codes, for example American Concrete Institute (ACI) 440,[18] Canadian Highway Bridge Design Code CHBDC,[19] Italian Standard CNR DT2005,[20] Japanese Society of Civil Engineers (JSCE),[21] Norwegian Standard NS 3473[22] and the STF 22A98741[23] propose two separate reduction factors taking into account the deterioration caused by environmental and long-term effects.

It is worth mentioning that the combined effects of environmental deterioration and sustained loads are considered by multiplying together the two load factors, which can result in very low permissible stresses.

It is clear that these differences in design approach to FRP durability make it difficult for the international construction community to have confidence in predictions of FRP service life in aggressive environments. Consequently, a more rigorous approach to durability specification needs to be adopted.

FIB[10] presents a new methodology which takes into account all the environmental influences on FRP and allows engineers to choose more realistic margins of safety. It is proposed that aramid fibres can be designed for durability on the basis of a simple strength equation. The characteristic long-term strength f_{fk} of fibres is linked to the characteristic short-term strength f_{fk0} by the following equation

$$f_{fk} = f_{fk0}/\eta_{env,t} \quad (1)$$

The long-term strength f_{fk} is affected by environmental and time effects, for example moisture, alkali, temperature and creep, while the short-term strength f_{fk0} has no such effects. The value of the environmental strength reduction factor $\eta_{env,t}$ depends on the severity of the exposure environment.

$\eta_{env,t}$ can be determined[24] accurately if the 1000 h tensile strength $f_{fk1000h}$ is known and it is assumed that the strength reduction continues at the same rate on a logarithmic time scale. R_{10} is the standard reduction of tensile strength in percent per logarithmic decade (i.e. slope of Figure 3).

$$\eta_{env,t} = f_{fk0}/\{f_{fk\,1000h}[(100 - R_{10})/100]^n\} \quad (2)$$

If $f_{fk1000h}$ is not known, the above approach is modified by Weber[25] and the following equation is recommended

$$\eta_{env,t} = 1/[(100 - R_{10})/100]^{n+2} \quad (3)$$

The exponent n in these equations is the sum of four influence terms.

$$n = n_{mo} + n_T + n_{SL} + n_d \quad (4)$$

Details of these influence terms are given elsewhere.[10] The

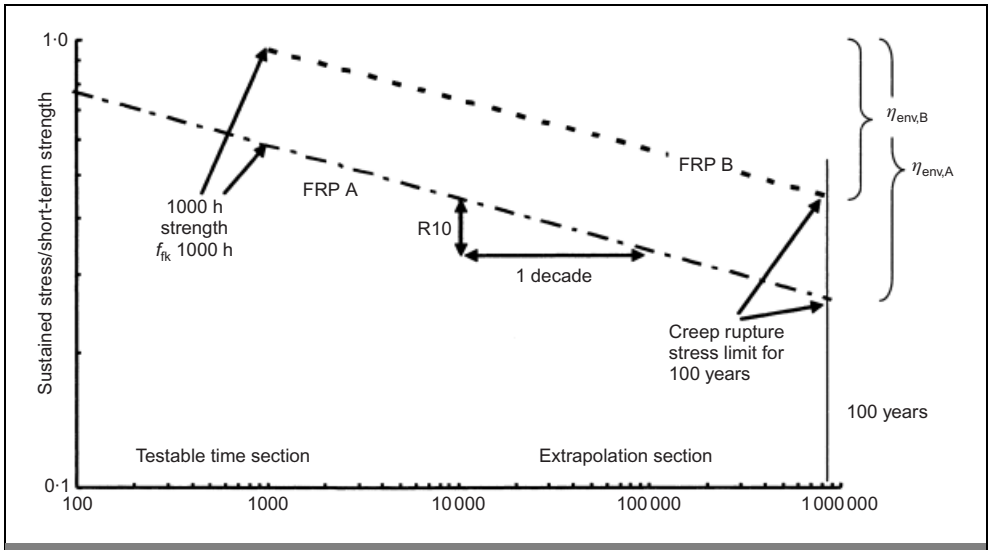

Figure 3. Environmental strength reduction factor and 1000 h strength for two FRP materials with different durability[10]

exponent n for standard exposure conditions is 3 as shown in Table 3.

This paper examines the long-term stress–rupture behaviour of aramids, using new test results on Kevlar 49 and Technora yarns. These data, obtained at low stress levels, albeit using an accelerated testing procedure, give more assurance that the extrapolations to structural lifetimes can be carried out with greater confidence, without the application of penalising high factors of safety. Therefore, stress limits for a service life of 50 or 100 years are proposed for aramid fibres and compared with the values reported in literature and in existing international design guidelines.

3. CREEP TESTS ON ARAMID FIBRES

The creep data used in this paper are part of a larger study[26,27,29] into the stress–rupture behaviour of Kevlar 49 and Technora. This study includes conventional creep tests at ambient conditions and accelerated tests at elevated temperatures and stress levels, using the stepped isothermal method (SIM)[26–28] and the stepped isostress method (SSM).[26,29]

Kevlar 49 is an aramid fibre made by Du Pont,[30] from a single monomer unit. Technora is a copolymer, made by Teijin[31] using a slightly different process. One of the monomer units is the same as that in Kevlar 49, but the other is different. Both fibres obtain their high strength from the natural axial alignment of the polymer chain and hydrogen bonding between adjacent molecules, which encourages the formation of aligned liquid crystals.

Kevlar 49 and Technora yarns, available in reel forms, were used for all tests. The cross-sectional area (A) of the yarns, after removing moisture, was found to be 0·17497 mm^2 and 0·12260 mm^2 respectively. The breaking load of Kevlar 49 and Technora was determined from 20 short-term tensile tests. From the dispersion of results a mean value μ_p and a standard deviation σ_p were determined. The measured values shown in Table 4 are in agreement with the values given by the two manufacturers.[30,31]

Conventional creep tests (CCTs) at different stress levels (77·5–95% ABL) were carried out in a special room under constant temperature (25°C) and humidity (50% RH) on both materials. Each specimen was subjected to a constant load by hanging dead-weights from the bottom clamp. Four tests were performed at each load level and failure of the specimens was achieved in a reasonable time scale (a few months).

SIM tests and SSM tests for Kevlar 49 and Technora yarns at different load levels (50–80% ABL) were carried out. Eight tests using SIM and four tests using SSM were conducted at each load level. Experiments were not conducted below 50% ABL, since Kevlar 49 and Technora show a non-linear viscoelastic behaviour below 40% ABL[26,32] and the use of the superposition principle would not have been valid. A detailed description of the tests is presented elsewhere[26] but the methods are summarised below.

Material	Mean value μ_P: N	Standard deviation σ_P: N
Kevlar 49	444·60	8·22
Technora	349·01	6·75

Table 4. Mean value μ_p and standard deviation σ_p of the breaking load for Kevlar 49 and Technora

Variable	Dependency	Standard conditions	Value at standard conditions	Test conditions	Value at test conditions
n_{mo}	Moisture	80% RH	0·0	50% RH	−1·0
n_T	Temperature	5–15°C	0·0	25°C	1·0
n_{SL}	Service life	100 years	3·0	50 years	2·7
n_d	Diameter	As tested	0·0	As tested	0·0

Table 3. Four influence terms as standard and test conditions

3.1. Stepped isothermal method (SIM)

SIM testing involves loading a single specimen, under constant loads, with the *temperature* increased in a series of steps to accelerate the creep. Careful choice of temperature step and step duration allows the test to be completed in about 24 h. At each temperature step a creep curve (strain against time) is obtained; these are then adjusted to compensate for the different temperature levels and a creep master curve at a reference temperature is produced. The *activation energy* of the viscoelastic materials can be determined. SIM is, in essence, an extension of the time–temperature superposition (TTSP) method, which is well established for Arrhenius materials.

3.2. Stepped isostress method (SSM)

In SSM testing, a similar approach is adopted but the acceleration is obtained by increasing the *stress* in steps while keeping the temperature constant. Additional stress provides energy to the system in an analogue of the effect of heat in SIM. The equivalent to activation energy becomes a term with the units of volume, so an *activation volume* is obtained.

The creep master curves for Kevlar 49 and Technora, obtained from SIM and SSM testing at all load levels, match both in form and position, with a small scatter, showing the repeatability and equivalence of the two methods. Additionally, the curves were compared with the corresponding conventional creep curves obtained at ambient conditions and they match reasonably closely, which demonstrates that the SIM and SSM techniques are applicable here.[26,27,29]

All tests have been carried out until failure of the specimens. Therefore a complete set of stress–rupture data from conventional and accelerated creep tests is available for Kevlar 49 (111 tests) and Technora yarns (98 tests). The lifetime distribution is most simply shown by plots of applied load level against logarithmic time to failure (rupture time), as shown in Figures 4 and 5.

4. ANALYSIS OF CREEP DATA

It is observed from Figures 4 and 5 that for load levels between 50 and 95% ABL there is a linear increase of the logarithmic rupture time with decreasing applied load. This implies that the

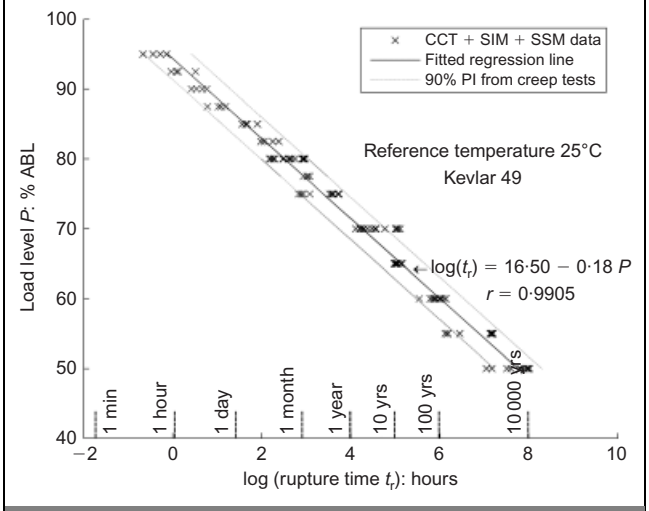

Figure 4. Rupture times from CCT, SIM and SSM tests with 90% prediction interval for Kevlar 49

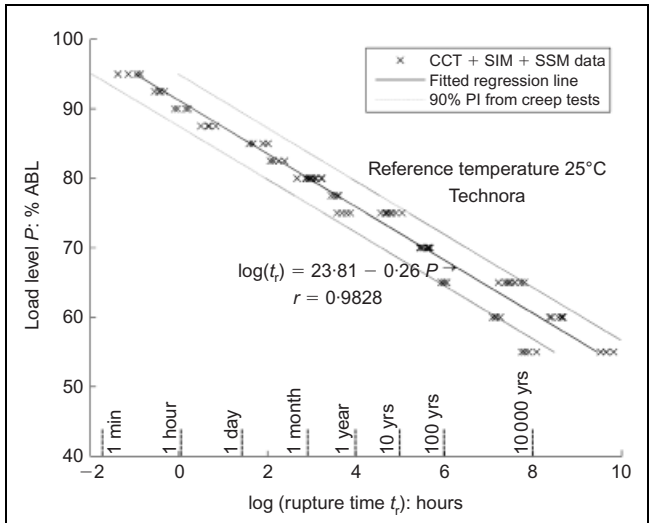

Figure 5. Rupture times from CCT, SIM and SSM tests with 90% prediction interval for Technora

data follow a lognormal distribution, which can be modelled using a lognormal regression analysis. Many researchers[12,33–36] have used lognormal distributions to analyse life data; the validity of this model will be discussed below.

The lognormal regression analysis relates a dependent variable $f(x)$ (here the load P) to an independent variable x (log (rupture times)).

The probability density function is defined by[37]

$$f(x;\mu,\sigma)=\frac{1}{x\sigma\sqrt{2\pi}}e^{(\log(x)-\mu)^2/2\sigma^2} \quad (5)$$

where
x is the independent variable ($x > 0$)
σ is the mean value
μ is the standard deviation

Several ways are available to check the conformity of a lognormal distribution; histogram, kernel density estimator, lognormal probability plot and Lilliefors test. More details for the application of those tests are given elsewhere.[26]

5. RESULTS AND DISCUSSION

Creep data for Kevlar 49 and Technora were fitted to a lognormal distribution and the test methods described above were used to check the validity of the model. From Figures 6 and 7 for Kevlar 49 and Technora respectively, it can be observed that the two histograms and kernel density plots have a bell shape, indicating the normality of the two data sets. Also, the points on the lognormal probability plots form a nearly linear pattern, which indicates that the lognormal distribution is a good model for these data sets. Finally, the two creep data sets were checked using Lilliefors test, which also confirmed that the data were lognormal.

The two fitted lognormal regression lines to the creep test data of the two materials shown in Figures 4 and 5 are

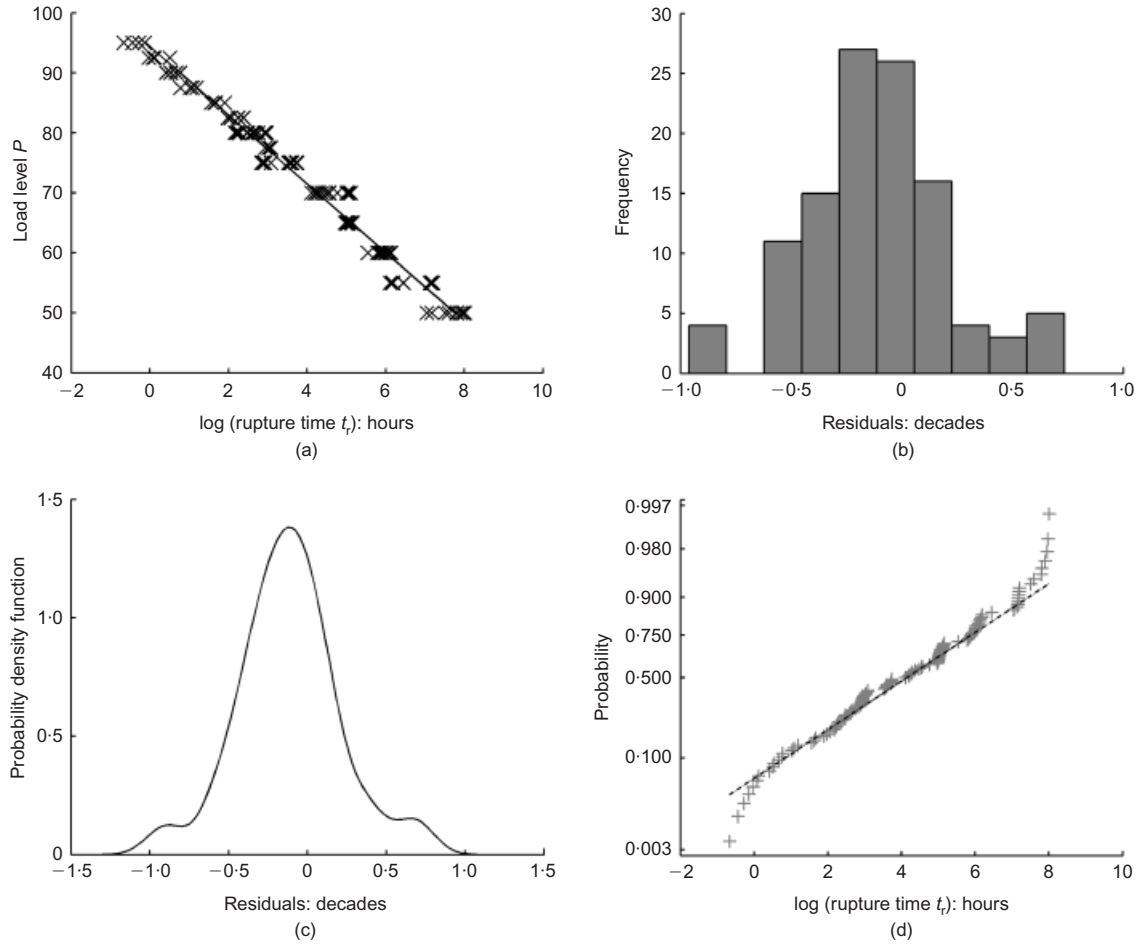

Figure 6. Lognormal distribution and validity checks of creep data for Kevlar 49: (a) creep data for Kevlar 49; (b) histogram; (c) kernel density population; (d) lognormal probability

6	$\log(t_r) = 16{\cdot}50 - 0{\cdot}18P$ for Kevlar 49

7	$\log(t_r) = 23{\cdot}81 - 0{\cdot}26P$ for Technora

where t_r is rupture time in hours and P is the load expressed as a percentage of ABL.

The variation of the test data at all load levels about the two fitted regression lines is small ($r = 0{\cdot}9905$ and $r = 0{\cdot}9828$ for Kevlar 49 and Technora respectively).

The objective of this analysis is to produce a curve for mean time to failure and two curves corresponding to 5 and 95% confidence limits. Using the creep test data, the 90% prediction interval (PI) of the regression line is calculated and plotted also in Figures 4 and 5. As the 90% prediction interval (PI) is the area in which 90% of all data points are expected to fall, that is 5% above and 5% below, then the lower 90% prediction interval line is also the 95% characteristic curve for the material. For Kevlar 49, only $0{\cdot}05 \times 111 = 5{\cdot}55$ points are expected to fall below the lower 90% PI line and this is confirmed from Figure 4. A similar observation is obtained for Technora from Figure 5. The standard deviation in the logarithmic time to failure for Kevlar 49 is 0·32 decades, while for Technora it is 0·58 decades.

The characteristic value of the stress–rupture lifetime will be 1·645 standard deviations below the mean. The 90% PI lines are drawn in Figures 4 and 5 assuming that they have the same slope as the mean line (i.e. the standard deviation is constant both as the load changes or the log time to failure changes). Figure 8 shows how the standard deviation of the short-term strength (σ_P) can be compared with the standard deviation of the logarithmic rupture time ($\sigma_{\log(tr)}$), assuming a constant slope.

The constant slope and the constant standard deviation of the log rupture time would predict a short-term strength variability of 7·9 and 7·8 N for Kevlar 49 and Technora respectively. These values are in agreement with values in Table 4. A very useful conclusion that can therefore be deduced is that the dispersion in the logarithmic rupture time values under a constant axial load can be explained from the dispersion in the static breaking load values. An analogous conclusion was drawn for fatigue tests by Leeuwen and Siemes[38] and Holmen.[39]

Figures 4 and 5 allow conclusions to be drawn about the variability of the two fibres. The vertical difference between the 5% and 95% confidence limits is 7·9 N for Kevlar 49 and 7·8 N for Technora, but they have different short-term strengths, which correspond to coefficients of variation of 1·8% for Kevlar and 2·2% for Technora. Because of the difference in the slope of the stress–rupture curves (which can be related to the activation energy of the materials) the effect of variability in

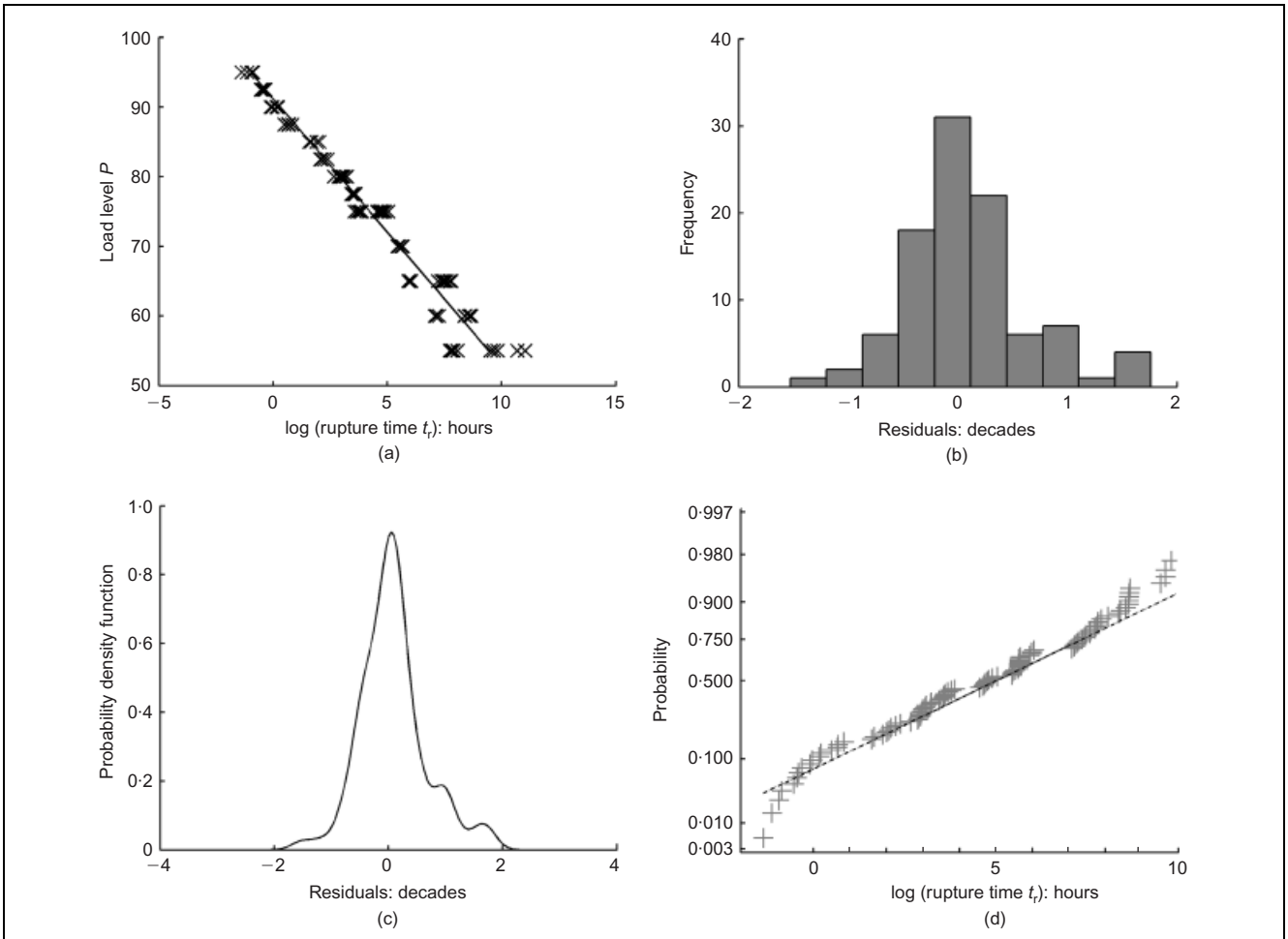

Figure 7. Lognormal distribution and validity checks of creep data for Technora: (a) creep data for Technora; (b) histogram; (c) kernel density population; (d) lognormal probability

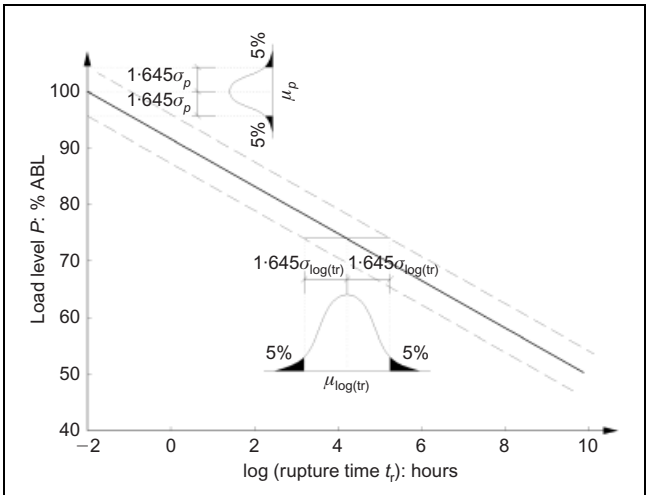

Figure 8. Relation between the dispersion in the static breaking load values and the rupture time values

the fibres is more pronounced for Technora when considering the horizontal shifting between the 5% and 95% characteristic lines. For Kevlar, this offset is 0·52 decades of the log time scale, while for Technora is 0·95 decades.

The 95% characteristic curves for Kevlar 49 and Technora can be used for design purposes as the characteristic strength f_{fk} for any prescribed design life. To obtain the design strength f_{fd} a material partial safety factor γ_f should be applied. Because no extrapolation is carried out, a less conservative factor can be applied than the one proposed in FIB. However, to obtain such a value a full reliability analysis would have to be carried out.[40,41] A simpler approach in many Japanese codes is adopted,[21] in which the use of a guaranteed strength f_{fd} is taken to be three standard deviations below the mean, which corresponds to a 99·73% PI line. This allows the use of a smaller partial safety factor than if the normal characteristic strength were used. For a design life of 50 years ($t_r = 50$ years) at 25°C, the resulting values are shown in Table 5.

These values correspond to a partial material safety factor of 1·04 applied to the characteristic value, and are of the same order as the values given in Table 1 by various researchers.

The design strength f_{fk} for a 50 year design life obtained from the creep data (Equations 6 and 7) can be compared with the stress limit obtained from the refined approach of FIB.[10] As

Material	f_{fk} (50 years): % ABL	f_{fd} (50 years): % ABL
Kevlar 49	58·6	56·3
Technora	65·8	63·1

Table 5. Characteristic and design strength values obtained from the current study

explained, the value of the environmental strength reduction factor $\eta_{env,t}$ can be calculated for the specific environmental conditions and for a prescribed design life. The terms for moisture condition, temperature, service life and diameter of specimen are 50% RH, 25°C, 50 years and the same size as tested respectively. Therefore, the influence factor n is 2·7, as shown in Table 3.

In addition, the characteristic strength at 0 and 1000 h and the slope R10 for the two materials from Figures 4 and 5 are given in Table 6.

Following the refined approach of FIB[10] and using Equations 1 and 2, the following $\eta_{env,t}$, $f_{fk(50yrs)}$ and $f_{fd(50yrs)}$ values are obtained for the two materials (Table 7).

The design strength values (Table 7) are lower than the values obtained from the current study (Table 5), showing that the FIB approach is more conservative than the current results. This was expected, as FIB is extrapolating creep data at 1000 h to predict the stress–rupture behaviour after 50 years and a penalising partial factor ($\gamma_f = 1{\cdot}25$) owing to uncertainties had to be applied (Figure 9). In the current study, data are available at lower load levels and therefore a less conservative partial factor can be applied ($\gamma_f = 1{\cdot}04$).

Material	f_{tk0}	f_{fk1000}	R_{10}
	% ABL		
Kevlar 49	96·85	73·94	5·6
Technora	96·82	76·41	3·7

Table 6. Characteristic strength at 0 and 1000 h and slope R_{10}

Material	$\eta_{env,t}$	f_{fk} (50 years): % ABL	f_{fd} (50 years): % ABL
Kevlar 49	1·52	63·7	51·0
Technora	1·40	69·2	55·4

Table 7. Characteristic and design strength values obtained from FIB approach

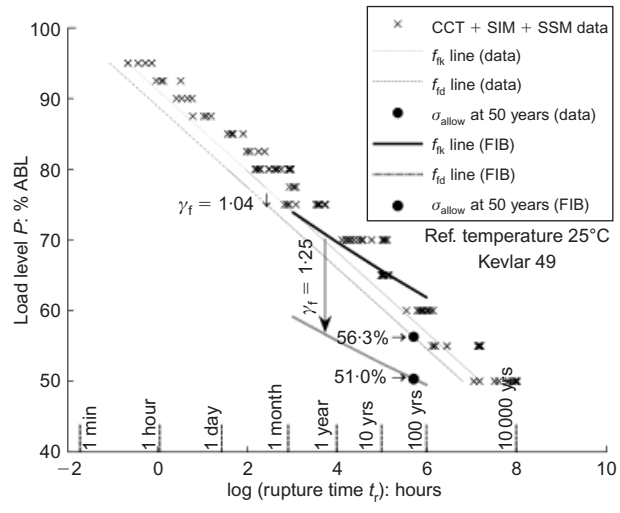

Figure 9. Design strength obtained from current data and from FIB approach for a 50 years design life for Kevlar 49

5.1. Effect of temperature

It should be pointed out that the fitted regression lines for Kevlar 49 and Technora, shown in Figures 4 and 5 respectively, have been obtained for a reference temperature of 25°C. It is possible to shift these lines to correspond to a different temperature T. The amount of shift $\log(\alpha_T)$ is determined from the Arrhenius equation[42]

$$\log(\alpha_T) = \frac{E}{2{\cdot}30R}\left(\frac{1}{T} - \frac{1}{T_R}\right) \quad (8)$$

where
E is the activation energy of the reaction (J/mol)
h is the universal gas constant (= 8·314 J/K per mol)
T is the temperature (K)
T_R is the reference temperature (K)

Activation energies for Kevlar 49 and Technora were determined during the SIM testing and found to be 119 and 138·6 kJ/mol respectively.[26,27]

By inserting the above equation into the stress–rupture equations (Equations 6 and 7) new relationships are obtained, which take account of the temperature for Kevlar 49:

$$\log(t_r) = -4{\cdot}54 + \frac{6270}{T} - 0{\cdot}18\,P \quad (9)$$

and similarly for Technora:

$$\log(t_r) = 0{\cdot}51 + \frac{7248}{T} - 0{\cdot}26\,P \quad (10)$$

Applying the above relationships, load–log (rupture times) lines are determined at four different reference temperatures (0, 25, 40, 60°C) as shown in Figures 11 and 12 for the two

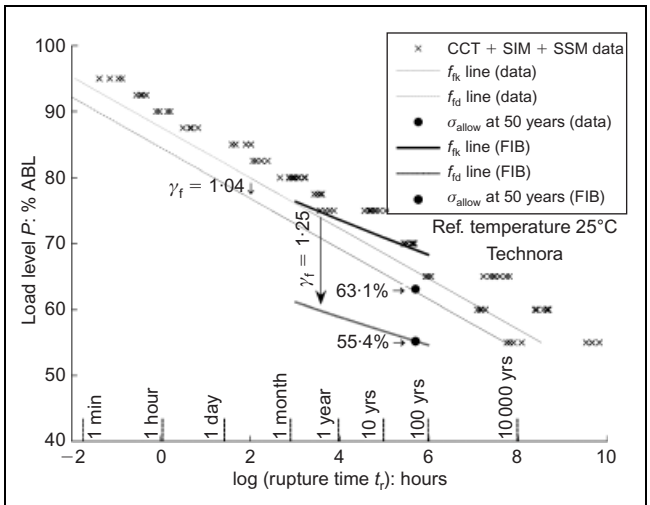

Figure 10. Design strength obtained from current data and from FIB approach for a 50 years design life for Technora

materials. Increasing the reference temperature decreases the rupture time as expected.

6. CASE STUDY

The load–rupture curves given in Figures 11 and 12 are for various constant reference temperatures. In reality the temperature during the design life (50 or 100 years) of a structure does not remain constant. Large temperature variations occur from day to night and from winter to summer, which affect the rupture time.

Because of these temperature variations there is cumulative damage and the total damage for any constant load level P is assumed to be the sum of the damage contributions from the temperature at each time interval[43]

$$\sum_{i=1}^{n} \frac{T_i}{(t_r)_i} \qquad (11)$$

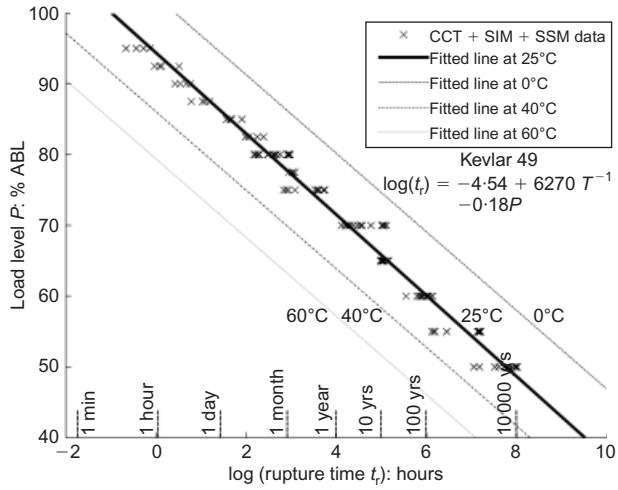

Figure 11. Load–rupture times for Kevlar 49 yarns at various reference temperatures

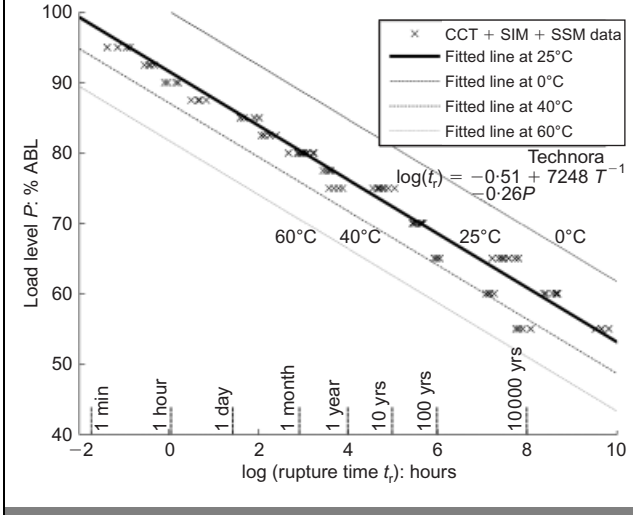

Figure 12. Load–rupture times for Technora yarns at various reference temperatures

where
T_i is the temperature applied at the ith time interval
$(t_r)_i$ is the rupture time corresponding to the temperature T_i, which can be determined from Equations 9 or 10
n is the number of constant time intervals Δt

Therefore, given a temperature profile for a long period of time, an equivalent constant temperature (T_{eff}) can be determined which induces the same damage.

$$\sum_{i=1}^{n} \frac{T_i}{(t_r)_i} = \frac{T_{eff}}{(t_r)_{eff}} \qquad (12)$$

By inserting Equations 9 or 10 into Equation 16 it can be shown that T_{eff} is independent of the applied load.

It is now possible to determine the maximum allowable load for a given temperature profile and a given design life. T_{eff} is first determined from the temperature profile, and then Equations 9 or 10 can be used to determine the limiting load for a given design life.

This approach will be applied to show how the safe load capacity can be determined if aramid cables were to be used in a real structure. For this purpose the temperature profile of the new Rio-Antirion bridge is used. This is a cable-stayed bridge crossing the Gulf of Corinth near Patras (200 km west of Athens), linking the town of Rio on the Peloponnese to Antirion on mainland Greece. It is a five-span four-pylon cable-stayed bridge with a total length of 2252 m (Figure 13).

A typical temperature profile for Rio-Antirion Bridge during has been made available to the authors (personal communication, A. Gefyra, 2008). Temperature sensors were placed on the deck close to pier M3; they were housed in ventilated enclosures to shade their sensor from direct sunlight, thereby allowing them to measure the air temperature in the shade. The temperature profile, over one year (2006), is shown in Figure 14; readings were taken every 2 h.

The given profile is divided into time intervals. The damage contribution from the temperature during each time interval, given by $T_i/(t_r)_i$, is shown in Figure 15 for $P = 50\%$ ABL. Sudden peaks are observed during hot days since the numerator of the fraction becomes rather high while the denominator becomes rather small.

Equation 12 can be solved numerically using a suitable program (e.g. Matlab) for the one unknown parameter T_{eff}, introducing the temperature profile data from Figure 14 and Equation 9 or 10. A value of $T_{eff} = 21{\cdot}84°C$ was calculated when using a 2 h time interval. Alternatively, using 1 day time interval a value of $T_{eff} = 21{\cdot}28°C$ was obtained.

It should be noted that the given one-year temperature profile is for conditions under shade. If aramid ropes are used as bridge stay cables the following points must be considered.

(*a*) The ropes are exposed to the full sunlight for a few hours every day. Therefore, the temperature profile must be modified accordingly.

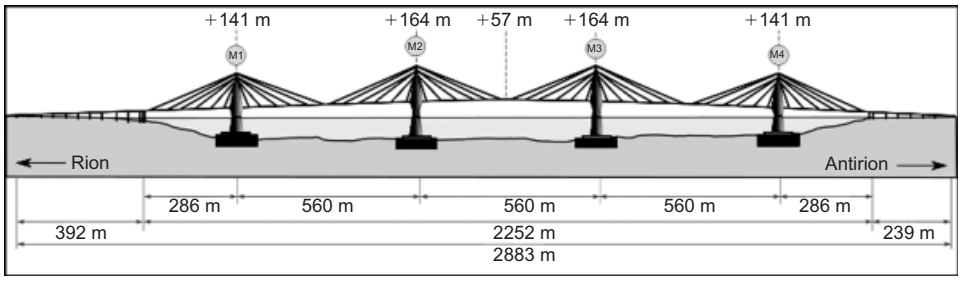

Figure 13. Elevation chart of the Rio-Antirion Bridge

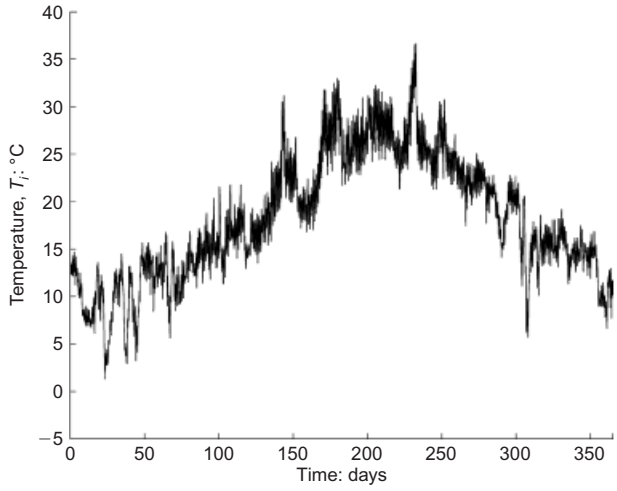

Figure 14. A typical temperature profile during a year for Rio-Antirion Bridge with readings taken every 2 h

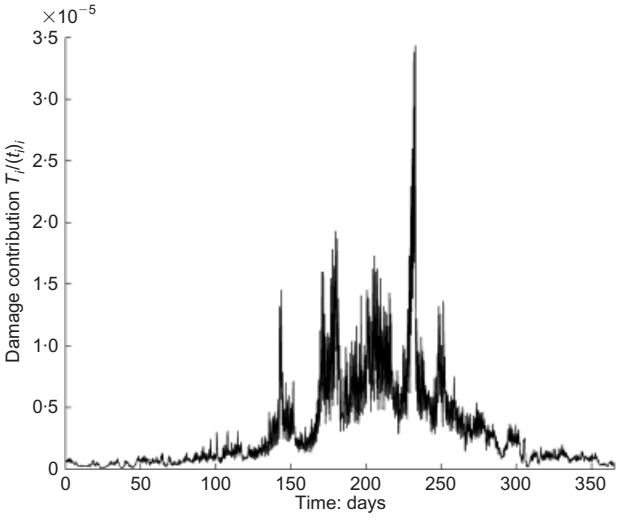

Figure 15. Damage contribution from the temperature for each 2 h time interval for Rio-Antirion Bridge

(*b*) The ropes are positioned inside a rather thick polyvinyl chloride (PVC) protection sheath. This results in temperature differences inside and outside the tube, which are affected by the material, the thickness and the outside colour of the material of the sheath. This is normally black, to ensure no UV penetration, but white or coloured sheaths are available. No particular data are available for the temperature difference across the sheath, but general data for different coloured surfaces exist. Berg and Quinn[44] reported that, in mid-summer, white roads are almost the same temperature as the ambient, while black roads are approximately 11°C warmer than the air. Santamouris *et al.*[45] report asphalt temperatures close to 63°C and white pavements close to 45°C.

(*c*) Owing to the very low conductivity of Kevlar 49[30] and Technora[31] fibres, the outer fibres of the stay cables will be affected by daily external temperature variations, while the inner fibres will see much smaller variations.

Taking these factors into account, the given shade temperature profile is modified by increasing the temperature by an additional 1°C every hour between 08:00 and 14:00, and then decreasing it by the same amount until 20:00. Using this modified temperature profile in Equation 12 gives a value of modified T_{eff} of 23·7°C. This value is higher than that from the shade temperature profile by only 1·8°C. It can thus be concluded that it is reasonable to use the 25°C curve for design purposes, even when the cable will be subjected to occasional higher temperature excursions.

7. CONCLUSIONS

This paper has shown that it is possible to conduct accelerated tests on organic fibres which allow the long-term creep rupture behaviour to be established with confidence. These stepped isothermal method and stepped isostress method tests are shown to give good agreement with conventional creep testing but can be carried out much more rapidly, and at lower stress levels where conventional creep testing to failure is impractical. The effect is that it is now possible to predict lifetimes of these fibres, and of ropes or tendons made from them, with much more certainty than was hitherto possible.

The methods have been applied to two aramid fibres, which are similar but have slightly different chemical and physical structures. The results have shown that these differences do indeed get reflected in the long-term properties of the materials. It has been shown that Technora has more variability than Kevlar 49, and a higher viscoelastic activation energy, which means that it is less likely to be affected by stress–rupture at practical stress levels.

It has been shown that the test data can be used to predict allowable stresses for these materials in applications where they are subjected to high permanent stresses, the most obvious examples of which are prestressing tendons and bridge stay cables.

The methods by which the effects of temperature can be taken into account have been studied by using the measured

temperature profile from a bridge in a sunny location in Greece, in such a way that allowance can be made for the higher summer temperatures.

It is now possible to make use of these exciting materials in applications where lack of material knowledge has made engineers overly cautious about their use.

REFERENCES

1. BURGOYNE C. J. Advanced composites in civil engineering in Europe. *Structural Engineering International*, 1999, **99**, No. 4, 267–273.
2. BURGOYNE C. J. Aramid fibres for civil engineering applications. *Construction Materials Reference Book* (DORAN D. K. (ed.)). Butterworths, 1992.
3. ABELES P. W. and BARDHAN-ROY B. K. Prestressed concrete designer's handbook. *Viewpoint*, Slough, UK, 1981.
4. BURGOYNE C. J. (1993). Parafil ropes for prestressing applications. Chapter in *Fibre Reinforcing for Concrete Structures: Properties and Applications* (NANNI A. (ed.)). Elsevier, 1993, pp. 333–354
5. BALAFAS I. and BURGOYNE C. J. Optimal cost design for beams prestressed with FRP tendons. *Proceedings of the 6th International Conference on Fibre Reinforced Polymers for Reinforced Concrete Structures (FRPRCS-6), Singapore*, 2003, pp. 1391–1400.
6. ROSTASY F. S. and SCHEIBE M. Engineering model for forecast of stress rupture strength of stressed aramid fiber reinforced polymer bars embedded in concrete. *ACI, Special publication*, 1999, **188**, 1049–1062.
7. Fibre reinforced plastics in civil engineering structures, Gouda NL, 2003, CUR Recommendation 96.
8. BAU-ÜBERWACHUNGSVEREIN. *Load Supporting Plastic Members in Construction*. BUV, Germany, 2002.
9. COMITÉ EUROPÉEN DE NORMALISATION. *EN 13706: Reinforced Plastics Composites—Specifications for Pultruded Profiles*. CEN, Brussels, 2002.
10. INTERNATIONAL FEDERATION FOR STRUCTURAL CONCRETE. FRP reinforcement in RC structures. *Bulletin 40*. fib, Lausanne, 2007.
11. FERER K. M. and SWENSON R. C. *Aramid Fibre for Use as Oceanographic Strength Members*. Naval Research Laboratory, Washington, DC, 1976.
12. GUIMARAES G. B. *Parallel-lay Aramid Ropes for Use in Structural Engineering*. PhD, University of London, 1988.
13. YAMAGUCHI T., KATO Y., NISHIMURA T. and UOMOTO T. Creep rupture of FRP rods made of aramid, carbon and glass fibers. *Proceedings of the 3rd International Symposium on Non-metallic Reinforcement for Concrete Structures (FRPRCS-3)*, 1997, **2**, 179–186.
14. ANDO N., MATSUKAWA T., HATTORI M. and MASHIMA M. Experimental studies of the long term tensile properties of FRP tendons. *Proceedings of the 3rd Internatinal Symposium on Non-metallic Reinforcement for Concrete Structures (FRPRCS-3)*, 1997, **2**, 203–210.
15. GERRITSE A. and TAERWE L. Recommended design aspects for concrete members pretensioned with aramid fiber reinforced polymers. *Proceedings of the 4th International Symposium on Fiber Reinforced Polymer Reinforcement for Reinforced Concrete Structures*, 1999, **ACI SP-188**, 829–841.
16. ALWIS K. G. N. C. and BURGOYNE C. J. Time–temperature superposition to determine the stress-rupture of aramid fibres. *Journal of Applied Composite Materials*, 2006, **13**, 249–264.
17. INSTITUTION OF STRUCTURAL ENGINEERS. *Interim Guidance on the Design of Reinforced Structures using Fibre Composite Reinforcement*. Seto Ltd, August 1999.
18. AMERICAN CONCRETE INSTITUTE *Guide for the Design and Construction of Concrete Reinforced with FRP Bars*. ACI, Detroit, 2006, ACI Committee 318, Report 440·1R-06.
19. CANADIAN STANDARDS ASSOCIATION. *CAN/CSA-S6-00: CHBDC, Canadian Highway Bridge Design Code*. CSA International, Rexdale, Ontario, Canada, 2000.
20. CNR DT. Istruzioni per la Progettazione, l'Esecuzione ed il Controllo di trutture realizzate con Calcestruzzo armato mediante Barre di Materiale Composito Fibrorinforzato, 2005.
21. JAPANESE SOCIETY OF CIVIL ENGINEERS. *Recommendations for Design and Construction of Concrete Structures using Continuous Fibre Reinforced Materials*. JSCE, Tokyo, Japan, 1997.
22. NORWEGIAN STANDARD. *Prosjektering av betongkonstruksjoner -Beregnings- og konstruksjonsregler*. NS 3473, 1998.
23. *Eurocrete Modifications to NS3473 when using FRP Reinforcement*. Norway, 1998, STF 22A98741 Report.
24. *DIN 53768. Extrapolation Method for the Prediction of the Long Term Behaviour*. Beuth Verlag Berlin, 1990.
25. WEBER A. Durability approach for GFRP rebars. *Proceedings.of the 3rd International Conference on FRP Composites in Civil Engineering, Miami*, 2006.
26. GIANNOPOULOS I. P. *Creep and Creep-Rupture Behaviour of Aramid Fibres*. PhD thesis, University of Cambridge, 2009.
27. GIANNOPOULOS I. P. and BURGOYNE C. J. Stepped isothermal method (SIM) test results for aramid fibres. *5th Conference on Advanced Composite Materials in Bridges and Structures (ACMBS-V), Winnipeg*, 2008, paper 79.
28. THORNTON J. S., ALLEN S. R., THOMAS R. W. and SANDRI D. The stepped isothermal method for TTS and its application to creep data on polyester yarn. *Sixth International Conference on Geosynthetics, Atlanta*, 1998.
29. GIANNOPOULOS I. P. and BURGOYNE C. J. Stepped isostress method for aramid fibres. *9th International Conference on Fibre Reinforced Polymers for Reinforced Concrete Structures (FRPRCS-9), Sydney*, 2009.
30. DU PONT. *Data Manual for Fibre Optics and other Cables*. E. I. Du Pont de Nemours and Co. (Inc.), 1991.
31. TEIJIN LIMITED High tenacity aramid fibre. *Technical Bulletin*. Teijin Limited, 1986.
32. ALWIS K. G. N. C. and BURGOYNE C. J. Viscoelasticity of aramid fibres. *Journal of Material Science*, 2008.
33. CHAMBERS J. J. *Parallel-lay Aramid Ropes for use as Tendons in Prestressing Concrete*. PhD thesis, University of London, 1986.
34. NELSON W. *Accelerating Testing, Statistical Models, Test Plans, and Data Analysis*. Wiley, New York, 1990.
35. DAVIES R. B., HALES R., HARMAN J. C and HOLDWORTH S. R. Statistical modelling of creep rupture data. *Journal of Engineering Material Technology*, 1999, **121**, 264—271.

36. ALWIS K. G. N. C. and BURGOYNE C. J. Statistical lifetime predictions for aramid fibres. *Journal of Composites in Construction*, 2005, **9**, No. 2, 106–116.
37. CROW E. L. and SHIMIZU K. *Lognormal Distributions: Theory and Application*. Dekker, New York, 1988.
38. VAN LEEUWEN J. and SIEMES A. J. M. Miner's rule with respect to plain concrete. *Heron*, 1979, **24**, No. 1, 1–34.
39. HOLMEN J. O. *Fatigue of Concrete by Constant and Variable Amplitude Loading*. PhD thesis, The Norwegian Institute of Technology, University of Trondheim, 1979.
40. COMITÉ EUROPÉEN DE NORMALISATION. *Basis of Structural Design*. CEN, Brussels, 2002, EN 1990.
41. GULVANESSIAN H., CALGARO J. A. and HOLICKY M. *Designer's Guide to EN 1990: Eurocode: Basis of Structural Design*. Thomas Telford, London, 2002.
42. ARRIDGE R. G. C. *Mechanics of Polymers*. Oxford University Press, London, 1975.
43. SCHIJVE J. *Fatigue of Structures and Materials*. Springer, New York, 2001.
44. BERG R. and QUINN W. Use of light colored surface to reduce seasonal thaw penetration beneath embankments on permafrost. *Proceedings of the 2nd International Symposium on Cold Regions Engineering, Alaska*, pp. 86–99.
45. SANTAMOURIS M. *et al*. On the impact of urban climate on the energy consumption of buildings. *Solar Energy*, 2001, **70**, No. 3, 201–216.